

**Use of Organic Precursors and Graphenes in the Controlled
Synthesis of Carbon-Containing Nanomaterials for Energy
Storage and Conversion**

Journal:	<i>Accounts of Chemical Research</i>
Manuscript ID:	ar-2012-001475.R2
Manuscript Type:	Article
Date Submitted by the Author:	03-Oct-2012
Complete List of Authors:	Yang, Shubin; Max Planck Institute for Polymer Research, Max-Planck-Institut für Polymerforschung Mainz, Germany, Bachman, Robert; The University of the South, Department of Chemistry Feng, Xinliang; Max-Planck Institute for Polymer Research, Synthetic Chemistry Mullen, Klaus; Max-Planck-Institute for Polymer Research,

SCHOLARONE™
Manuscripts

Use of Organic Precursors and Graphenes in the Controlled Synthesis of Carbon-Containing Nanomaterials for Energy Storage and Conversion

Shubin Yang⁺, Robert E. Bachman[‡], Xinliang Feng^{+#,}, Klaus Müllen^{+,*}*

⁺Max Planck Institute for Polymer Research, Ackermannweg 10, D-55128 Mainz, Germany

[‡]Department of Chemistry, The University of the South, 735 University Avenue, 37383,
Sewanee, TN, USA

[#] School of Chemistry and Chemical Engineering, Shanghai Jiao Tong University, 200240,
Shanghai, P. R. China

KEYWORDS: Graphene, nanomaterials, supercapacitor, lithium ion batteries, fuel cells

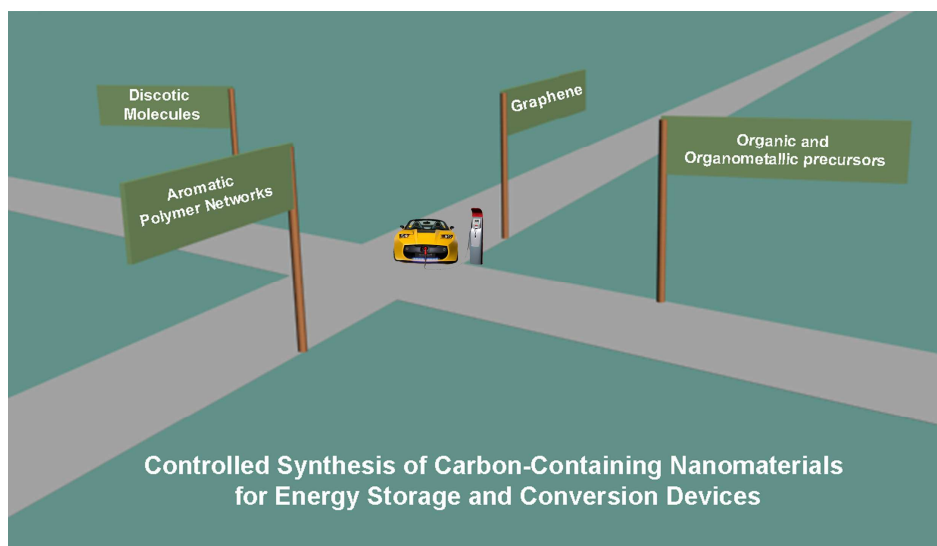
CONSPECTUS

The development of high-performance electrochemical energy storage and conversion devices, including supercapacitors, lithium-ion batteries and fuel cells, is an important step on the road to alternative energy technologies. Carbon-containing nanomaterials (CCNMs), defined here as pure carbon materials and carbon/metal (oxide, hydroxide) hybrids with structural features on the nanometer scale, show potential application in such devices. Because of their pronounced

1
2
3
4 electrochemical activity, high chemical/thermal stability and low cost, researchers are interested
5
6
7 in CCNMs to serve as electrodes in energy-related devices.

8
9
10 Various all-carbon materials are candidates for electrochemical energy storage and conversion
11
12 devices. Furthermore, carbon-based hybrid materials, which consist of a carbon component with
13
14 metal oxide or metal hydroxide-based nanostructures, offer the opportunity to combine the
15
16 attractive properties of these two components and tune the behavior of the resulting materials. As
17
18 such, the design and synthesis of CCNMs provide an attractive route for the construction of
19
20 high-performance electrode materials. Studies in these areas have revealed that both the
21
22 composition and the fabrication protocol employed in preparing CCNMs influence the
23
24 morphology and microstructure of the resulting material and its electrochemical performance.
25
26 Consequently, researchers have developed several synthesis strategies, including hard-templated,
27
28 soft-templated, and template-free synthesis of CCNMs.
29
30
31
32
33
34
35

36 In this Account, we focus on recent advances in the controlled synthesis of such CCNMs and the
37
38 potential of the resulting materials for energy storage or conversion applications. The Account
39
40 is divided into four major categories based on the carbon precursor employed in the synthesis:
41
42 low molecular weight organic or organometallic molecules, hyperbranched or cross-linked
43
44 polymers consisting of aromatic subunits, self-assembling discotic molecules, and graphenes.
45
46 In each case, we highlight representative examples of CCNMs with both new nanostructures and
47
48 electrochemical performance suitable for energy storage or conversion applications. In
49
50 addition, this Account provides an overall perspective on the current state of efforts aimed at the
51
52 controlled synthesis of CCNMs and identifies some of the remaining challenges.
53
54
55
56
57
58
59
60



TOC

1. Introduction

Fossil fuel depletion and global climate change present society with environmental and energy sustainability challenges.^{1,2} In response to these challenges there has been a strong push toward the adoption of electric vehicles (EVs) and hybrid EVs (HEVs) for transportation. However, a shift to such vehicles will require the development of more efficient portable energy storage and conversion devices.¹⁻⁴ Due to their energy and power densities, rechargeable lithium-ion batteries, supercapacitors/ultracapacitors and fuel cells are promising candidates to meet this need.² Since the performance of these devices depends intimately on the nature of the electrode materials, the development of new electrochemically active materials with high activities and robust structures has become an area of considerable research interest.^{5,6}

Pure carbon materials and carbon/metal (oxide, hydroxide) hybrids with nanometer scale structures, collectively referred to in this Account as carbon-containing nanomaterials (CCNMs), have become attractive as electrodes in energy-related devices because of their pronounced electrochemical activity, good electrical conductivity, high chemical/thermal stability and low

3

1
2
3
4 cost.⁷⁻⁹ Given the relationship between structural features and bulk properties in these materials,
5
6
7 it is worth clearly defining key structural terms at the outset. Specifically, the carbon component
8
9
10 in CCNMs can be categorized as either crystalline or amorphous based on the degree of
11
12 long-range structural order present. In the context of the electrode materials considered here,
13
14 amorphous carbon may be defined as consisting of local graphitic domains dispersed in a carbon
15
16 matrix with ill-defined long-range order.
17
18
19

20 Various all-carbon materials, with graphitic or amorphous structures, have been suggested as
21
22 candidates for electrochemical energy storage and conversion devices.⁷⁻¹⁰ Furthermore,
23
24 carbon-based hybrid materials, which combine a carbon component with metal (oxide or
25
26 hydroxide)-based nanostructures,^{11,12} offer the opportunity to combine the attractive properties of
27
28 the two components and thereby tune the behavior of the resulting materials for enhanced device
29
30 performance. As such, CCNMs seem to provide an attractive route for the construction of
31
32 high-performance electrode materials.^{7,13-15} Studies in these areas have revealed that not only the
33
34 composition but also the fabrication protocol employed in preparing CCNMs exerts a large
35
36 influence on the resulting electrochemical performance owing to its impact of the morphology,
37
38 microstructure and composition of the resulting material.¹⁶ Consequently, several strategies such
39
40 as hard-templated¹⁷, soft-templated¹³ and template-free synthesis¹⁵ of CCNMs have been
41
42 developed. In this Account, we summarize recent achievements, primarily focusing on our
43
44 contributions, toward the controlled synthesis of CCNMs for energy storage and conversion.
45
46
47 This Account is divided into four major sections guided by the type of precursor employed in the
48
49 preparation of the CCNMs: low molecular weight organic and organometallic precursors,^{18,19}
50
51
52
53
54
55
56
57
58
59
60

hyperbranched or cross-linked polymers with built-in aromatic subunits (defined as aromatic polymer networks here),^{15,20} discotic molecules capable of pre-organizations in the solid or liquid-crystalline state,^{7,21} and graphene sheets with varying degrees of oxidation.^{12,13,22}

2. Low molecular weight organic and organometallic precursors

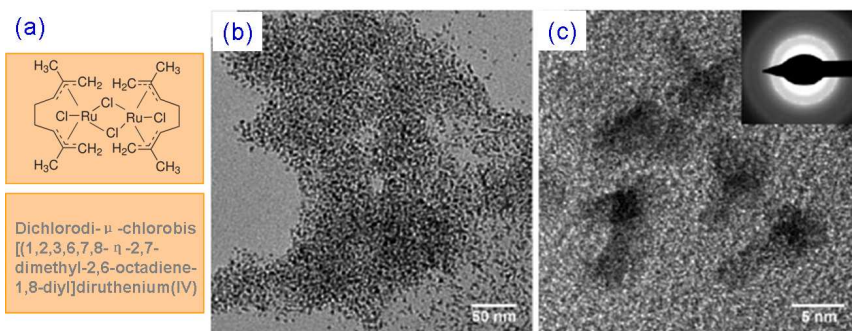


FIGURE 1. (a) Chemical structure of the Ru-containing precursor. (b) TEM and (c) HRTEM images of the carbon-Ru composite, with a selected area electron diffraction pattern shown in the insert.²³

Low molecular weight precursor molecules can be converted into CCNMs via pyrolysis, with or without the use of an additional structured template. While the chemical nature of the precursor employed in the pyrolysis process plays a dominant role in determining the composition, structure and function of the final CCNM, additional factors, such as the presence or absence of a template and the processing conditions, also play a role.

In 2007, we reported the pyrolysis of dichlorodi- μ -chlorobis [(1,2,3,6,7,8- η -2,7-dimethyl-2,6-octadiene-1,8-diyl]diruthenium(IV), at 700 °C (Figure 1) to yield a carbon-Ru composite. This CCNM was composed of crystalline Ru nanoparticles (3-7nm in diameter) homogeneously dispersed in a mesoporous amorphous carbon matrix.²³ The Ru

nanoparticles could subsequently be converted into RuO₂ via electro-oxidization in a sulfuric acid solution. The resulting carbon-RuO₂ composite functioned as supercapacitor, with a capacitance of 132 F g⁻¹ in 0.5 M H₂SO₄ electrolyte.²³ This value is comparable to that reported for carbon-RuO₂ composites prepared via a more complex multistep colloid-based synthesis.²⁴

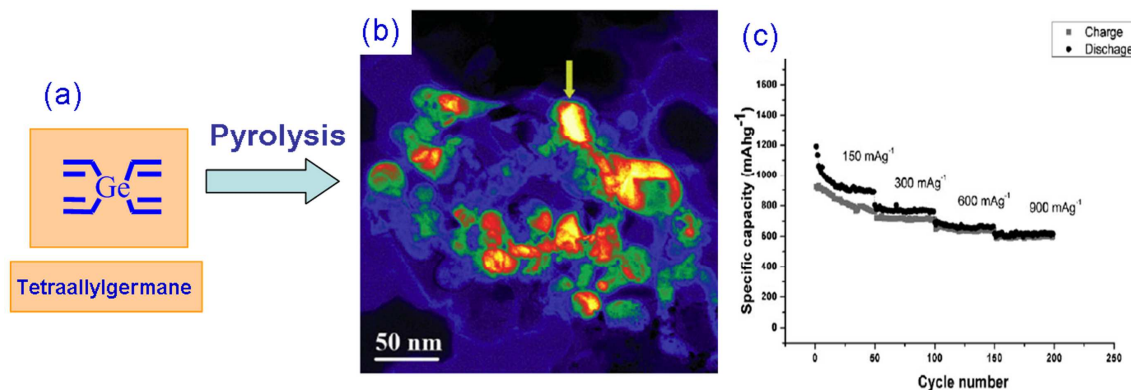


FIGURE 2. (a) Chemical structure of the tetraallylgermane precursor. (b) Elemental analysis of carbon-Ge composite. (c) Cycle and rate performances of carbon-Ge composite.¹⁸

Similarly, pyrolysis of other organometallic precursors, such as allyltriphenyltin¹⁹, tetraallylgermane¹⁸ or coordination complexes, such as cobalt acetylacetonate²⁵, also yield CCNMs (Figure 2). For example, pyrolysis tetraallylgermane generated a CCNM with 50 to 70 nm Ge nanoparticles homogeneously dispersed in an amorphous carbon matrix.¹⁸ The resulting carbon-Ge composite exhibited a reversible and stable charge capacity of approximately 900 mA h g⁻¹ at a current density of 150 mA g⁻¹. Furthermore, a capacity of 613 mA h g⁻¹ was achieved at the higher current density of 900 mA g⁻¹ (Figure 2c), which is much higher than that of electrodes contain only Ge nanoparticles (~200 mA h g⁻¹).¹⁸ The excellent electrochemical performance of this carbon-Ge composite can be attributed to several structural features. The small size of the Ge

1
2
3
4 nanoparticles reduces the lithium diffusion length during the cycling process to a few
5
6 nanometers. Additionally, the carbon matrix maintains a good electrical conductivity in the
7
8 electrodes while providing mechanical support and thereby preventing disintegration and/or
9
10 aggregation of the metal particles.
11
12

13
14
15
16 Despite the successful synthesis of various CCNMs via the template-free pyrolysis of
17
18 organometallic and coordination complex precursors, control of the bulk morphology as well as
19
20 the meso- and nano-scale structure of the CCNM products remains limited.^{18,23} In an attempt to
21
22 overcome these limitations, the use of inorganic templates during pyrolysis has been developed
23
24 in recent years. For instance, pyrolysis of butylcapped silicon in a SBA-15 silica template at
25
26 900°C generated mesoporous Si@C, consisting of Si@C nanowires (6.5 nm) and ordered
27
28 mesopores (2.3 nm) (Figure 3).²⁶ The resultant materials not only contained internal pores that
29
30 could be flooded with electrolyte, but also possessed core-shell Si-C nanowires, which are
31
32 favorable for the fast diffusion of lithium ions and the transfer of electrons.²⁶ As a consequence,
33
34 this Si@C composite exhibited a capacity of 3163 mAh g⁻¹ and stable cycle performance at 0.2C
35
36 for lithium storage. This capacity was about 8 times higher than that of commercial graphite
37
38 electrode (~300 mAh g⁻¹). More importantly, a capacity of 2462 mAh g⁻¹ at the higher rate of
39
40 2C could be achieved, representing an excellent high-rate performance for lithium storage.²⁶
41
42 Following this strategy, a series of CCNMs based on porous Si-C²⁷, Ge-C²⁸ nanocomposites and
43
44 core-shell Sn₇₈Ge₂₂-C²⁹, Si₉₀Ge₁₀-C³⁰ nanowires with high capacities above 1000 mAh g⁻¹ were
45
46
47
48
49
50
51
52
53
54
55
56 fabricated.
57
58
59
60

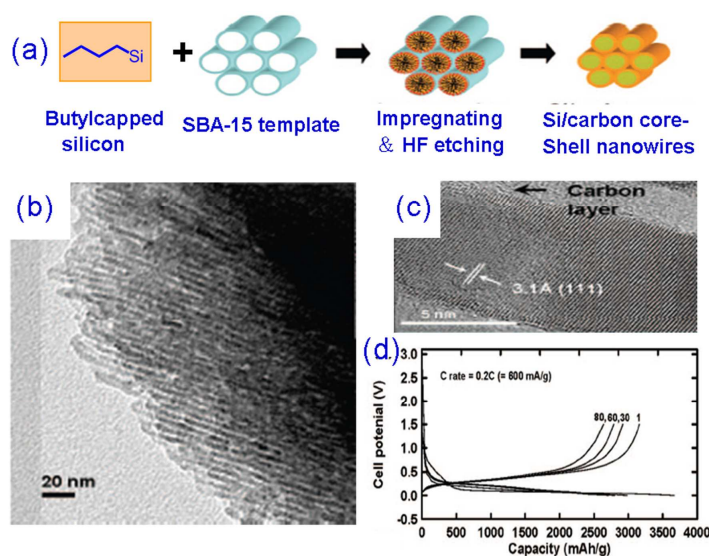


FIGURE 3. (a) Synthetic route to Si@carbon core-shell nanowires. (b) TEM and (c) HRTEM images of the Si@carbon nanowires. (d) Voltage profiles of the Si@carbon nanowire electrode at a rate of 0.2 C.²⁶

Heteroatom (N, B and P)-enriched CCNMs have also been fabricated by pyrolysis of molecular precursors.³¹ The incorporation of such heteroatoms can be used to tailor the electronic properties and chemical reactivity of resulting materials, and thereby give rise to new functions, such as electrocatalysis of the oxygen reduction reaction (ORR) required in fuel cells. For instance, pyrolysis of nucleobases dissolved in an ionic liquid (1-ethyl-3-methylimidazolium dicyanamide), yielded a nitrogen-doped porous carbon material with surface area of up to 1500 m² g⁻¹ (Figure 4).³² Applying silica nanoparticles as a template in this process produced a nitrogen-doped CCNM with nitrogen content as high as 12 wt % and a narrow mesopore size distribution centered at ~12 nm. The as-prepared material was capable of catalyzing the four-electron transfer process required of the ORR. Moreover, the observed low onset voltage for

oxygen reduction in alkaline medium and the high methanol tolerance of this CCNM are superior to those of commercial Pt/C catalysts³².

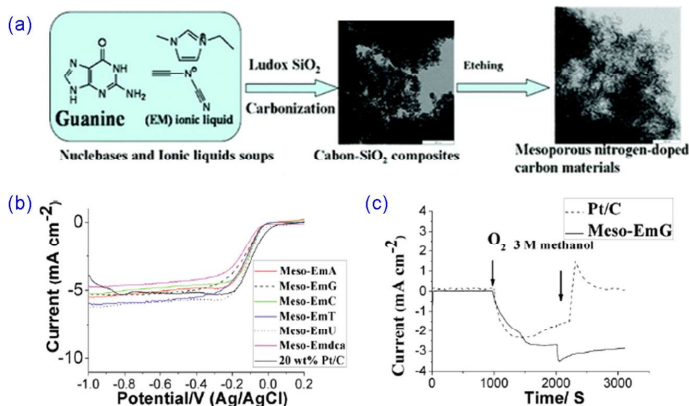


FIGURE 4. (a) Preparation of N-doped CCNMs as ORR catalysts. (b) RDE voltammograms of these materials. (c) Electrocatalytic selectivity among nitrogen, oxygen and methanol for the nitrogen-doped CCNM and Pt/carbon catalysts.³²

3. Aromatic polymer networks

Polymer networks with a rigid molecular backbone and a relatively fixed 3D architecture, such as hyperbranched polyphenylenes or cross-linked conjugated polyphenylene-ethnylene networks,³³⁻³⁵ provide another route for the synthesis of porous CCNMs. One advantage of such precursors in relation to the molecular precursors discussed above is their higher carbonization yields. Moreover, polymer precursors employed in preparing CCNMs can themselves be conveniently tailored by variation of the monomers employed and/or via adjustment of polymerization protocols. This flexibility allows one to control both the chemical composition and the solid-state structure of the polymer precursors, and hence the final CCNMs, at the molecular level.^{15,20}

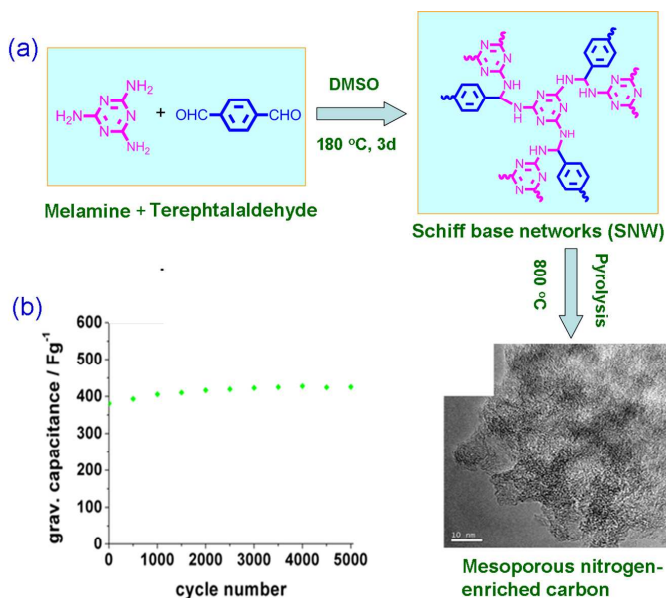


FIGURE 5. (a) Preparation of mesoporous nitrogen-enriched CCNMs. (b) Cycle performance of the CCNM in a 1M H₂SO₄ electrolyte at a current density of 2 A g⁻¹.¹⁶

For example, the one-pot A2B3-type polycondensation of melamine and terephthalaldehyde at 180°C in DMSO, generated a porous Schiff-base network. Subsequent pyrolysis of this network at 800°C provided a nitrogen-enriched CCNMs with mesoporosity, high surface area and tunable nitrogen content.¹⁶ This material exhibited a capacitance value of 381 F g⁻¹ in an acid electrolyte and 351 F g⁻¹ in an alkaline environment, with exceptionally stability over 5000 cycles (Figure 5)¹⁶. Both values are notably higher than those reported (100-200 F g⁻¹) for similar materials produced by methods which do not generate mesoporosity.¹⁶

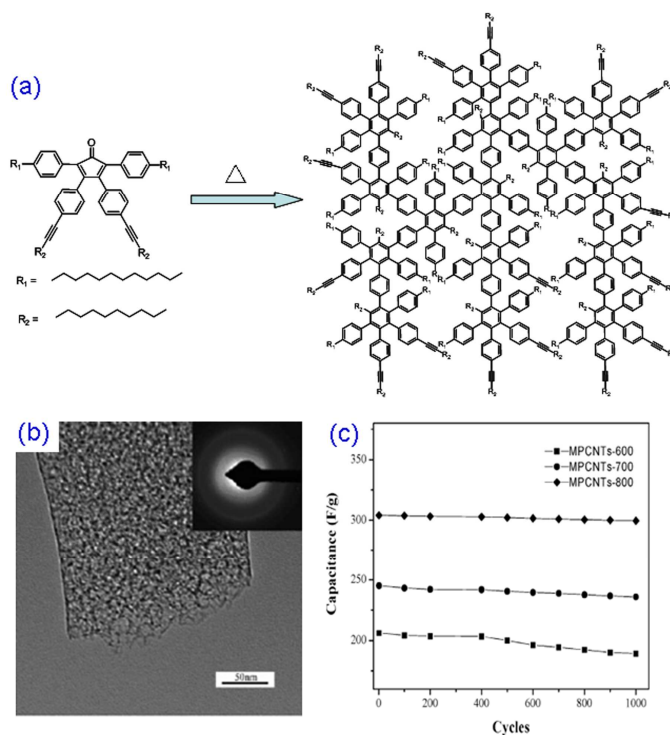


FIGURE 6. (a) Diels-Alder cycloaddition yielding a hyperbranched polyphenylene. (b) TEM image of the CCNM after pyrolysis. (c) Cycle performance of CCNMs from differing pyrolysis temperatures in 1 M H₂SO₄ electrolyte.³³

Another illustrative example is the pyrolysis of hyperbranched polyphenylene precursors obtained from an in situ thermally induced Diels-Alder reaction (Figure 6a). A typical AB₂-type (one diene and two dienophiles) functionalized cyclopentadienone (CP) was impregnated into the nanochannels of an anodic aluminum oxide (AAO) membrane. Upon thermal annealing at 250°C, alkyl-substituted hyperbranched polyphenylene was produced via intermolecular Diels-Alder reactions between the cyclopentadienone and alkyne moieties. Subsequent pyrolysis of the resulting polyphenylene precursor at 800°C generated a CCNM with 1D mesopores of between 10 and 20 nm and a surface area of 1140 m² g⁻¹.³³ The resulting material exhibited a capacitance of 304 F g⁻¹, with stable cycle performance in an acidic electrolyte (Figure 6).³³

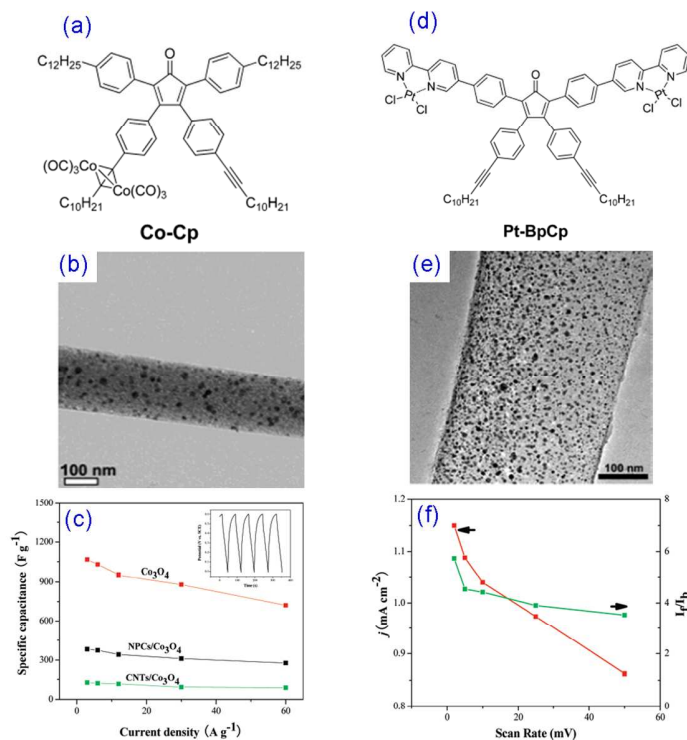


FIGURE 7. (a) Structure of Co-Cp. (b) TEM image of C- Co_3O_4 . (c) Capacitance vs. current density curves of C- Co_3O_4 , Co_3O_4 , and CNTs/ Co_3O_4 (inset: charge and discharge curves of C- Co_3O_4 at a density of 6 A g^{-1}). (d) Structure of Pt-BpCp. (e) TEM image of C-Pt. (f) Scan rate dependent current density (j) and I_f/I_b curves for the electro-oxidation of methanol on C-Pt.³⁴

This strategy was extended to fabricate CCNMs by pyrolysis of polyphenylene precursors with integrated metal complex moieties. For instance, AB2-type 3,4-bis(4-dodecynylphenyl)-2,5-bis(4-dodecylphenyl)cyclopentadienone and its corresponding $\text{Co}_2(\text{CO})_6$ complex (Co-Cp, Figure 7a) were used as monomers for the synthesis of cobalt functionalized polyphenylene skeletons via a Diels-Alder cycloaddition reactions. Pyrolysis of the resulting polymeric material produced a 1D porous CCNM consisting of amorphous carbon

1
2
3
4 and Co_3O_4 nanocrystals ($\text{C-Co}_3\text{O}_4$).³⁴ Similarly, a mixture of
5
6
7 3,4-bis(4-dodecynylphenyl)-2,5-bis(4-(2,2'-bipyridyl)phenyl) cyclopentadienone (BpCp) and its
8
9
10 corresponding platinum dichloride complex (Pt-BpCp, Figure 7d) allowed the synthesis of a
11
12 CCNM with Pt nanocrystals (C-Pt).³⁴ Structural characterizations revealed that the Co_3O_4 or Pt
13
14 nanocrystals were homogeneously dispersed within the carbon matrix. Moreover, these
15
16 carbon-metal (oxide) hybrids delivered excellent electrochemical performance for energy storage
17
18 or conversion. As shown in Figure 7, use of $\text{C-Co}_3\text{O}_4$ as an electrode material for a
19
20 supercapacitor, yielded a gravimetric capacitance of 1066 F g^{-1} , which ranks among the best
21
22 electrochemical capacitive values for cobalt oxide electrode materials.³⁴ Similarly, the C-Pt
23
24 showed a higher catalytic efficiency toward methanol oxidation than commercial Pt-based
25
26 materials when used as an electrocatalyst in fuel cells.³⁴
27
28
29
30
31
32
33
34
35

36 4. Self-assembling discotic molecules

37
38
39 Discotic molecules, such as porphyrin³⁶, perylene³⁷, hexa-*peri*-hexabenzocoronene (HBC)²¹
40
41 and their derivatives,²¹ are a unique class of carbon-rich molecules capable of self-assembling
42
43 into highly ordered columnar superstructures, and which frequently display liquid-crystalline
44
45 phase behavior. As such, such systems can be thought of as intermediate between the low
46
47 molecular weight molecular precursors and the polymer precursors discussed in the last two
48
49 sections. Discotic molecules tend to orient themselves in an edge-on manner on substrates such
50
51 as glass, polytetrafluoroethylene or highly oriented pyrolyzed graphite owing to their unique
52
53
54
55
56
57
58
59
60

1
2
3
4
5
6
7
8
9
10
11
12
13
14
15
16
17
18
19
20
21
22
23
24
25
26
27
28
29
30
31
32
33
34
35
36
37
38
39
40
41
42
43
44
45
46
47
48
49
50
51
52
53
54
55
56
57
58
59
60

supramolecular behavior, that is, a configuration that preserves internal aromatic π - π interactions at the expense of inhibited π -surface bonds.^{21,38} Consequently, pyrolysis of these discotic molecules typically results in the formation of graphitic carbon, as opposed to the amorphous materials discussed previously.⁷ For instance, pyrolysis of a branched alkyl substituted HBC at 600°C, with 3D porous inverse silica opal employed as a template, produced monodisperse graphitic microbeads with an orderly alignment.¹⁷ More interestingly, thermal treatment of (HBC-PhC12) in an alumina membrane (Figure 8a-8c) afforded carbon nanotubes in which the graphitic layers are oriented perpendicular to the surface of tube axis.²¹ This concept was adapted to fabricate hollow carbon spheres by employing HBC-C12 as the precursor and a silica/space/mesoporous-silica spheres as the template (Figure 8d-8f).⁷ The resulting hollow spheres exhibited uniform size and possessed dual walls, with a thicker, mesoporous exterior wall and thinner, solid interior wall. The nanochannels present in the exterior walls of the spheres are arranged perpendicularly to the surface spheres, which favors lithium ion diffusion, while the solid interior graphitic walls facilitate the collection and transport of electrons during electrochemical cycling (Figure 9). As a consequence, a reversible capacity (ca. 600 mAh g⁻¹) and high-rate capability (about 200 mAh g⁻¹ at the rate of 10 C) were achieved for lithium storage.⁷

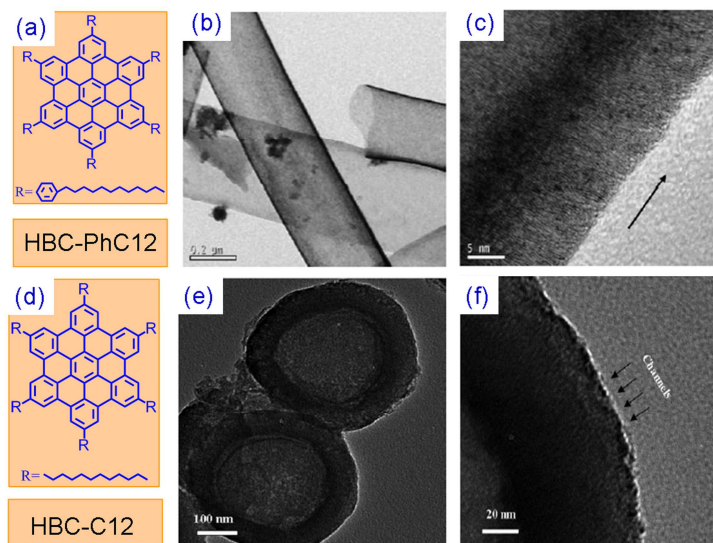


FIGURE 8. (a) Structure of HBC-Ph-C12. (b,c) HRTEM images of the CCNM showing the orientation of the graphitic layers in the tube wall.¹⁸ (d) Structure of HBC-C12. (e,f) HRTEM images of resulting hollow carbon spheres. The arrows denote the perpendicular arrangement of the surface nanochannels.⁷

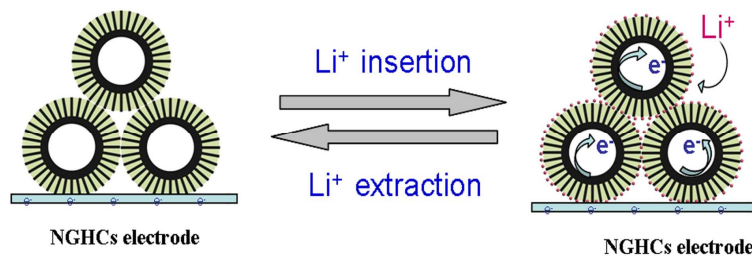


FIGURE 9. Diffusion of lithium ions and electrons during the electrochemical cycling of an electrode based on hollow carbon spheres produced from the templated pyrolysis of HBC-C12.⁷

Use of nitrogen-containing precursors, such as N,N'-bis(2,6-diisopropylphenyl)-3,4,9,10-perylenetetracarboxylic diimide (PDI) or tetrakis(tert-butyl) naphthalocyanine, and templates such as ordered mesoporous silica SBA-15 allowed for the fabrication of nitrogen-enriched CCNMs incorporating a nitrogen content of ~3 wt% in a mesoporous graphitic

1
2
3
4 carbon matrix (Figure 10).³⁹ These materials, which possess a surface area of $\sim 500 \text{ m}^2 \text{ g}^{-1}$,
5
6 function as a metal-free catalyst for the ORR, exhibiting high electrocatalytic activity and
7
8 long-term stability in alkaline conditions.³⁹ Indeed, the characteristics of these materials were
9
10 superior to those observed for commercially available Pt-C catalysts in terms of current density
11
12 and electron transfer number. Additionally, this work demonstrated the importance the presence
13
14 of graphite-like nitrogen for the electrocatalytic activity.³⁹
15
16
17
18
19
20

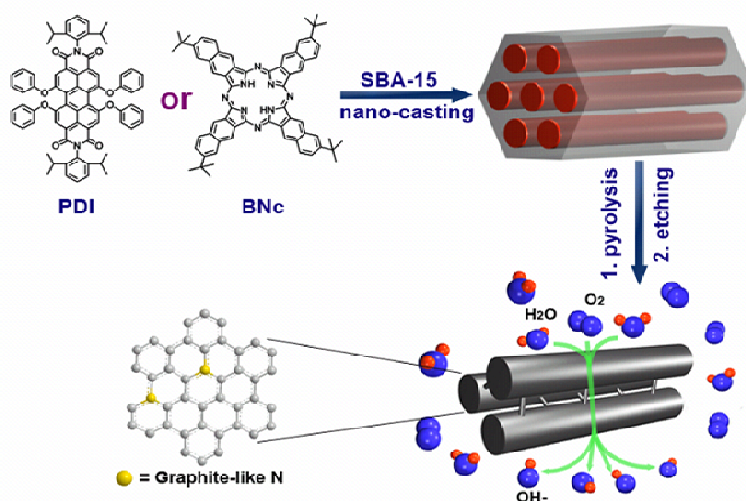


FIGURE 10. Preparation of nitrogen-enriched CCNMs as metal-free catalysts for ORR.³⁹

5. Graphene and graphene oxide sheets

Graphene, a 2D “aromatic” monolayer of carbon atoms, has attracted tremendous attention recently owing to its host of attractive physical properties, including superior electrical conductivity, large surface area, excellent mechanical flexibility, and high thermal/chemical stability.^{14,40-42} Various graphene-metal (oxide) composites such as graphene-Pt,⁴³ graphene-SnO₂,⁴⁴ graphene-Co₃O₄⁴⁵ and graphene-Mn₃O₄⁴⁶ have been reported. These materials

1
2
3
4 show enhanced electrochemical properties with respect to the corresponding metal (oxide)
5
6 systems by taking advantage of the additional properties provided by the graphene
7
8 component.^{14,45,46} In particular, graphene can provide a fast electron-transport pathway in the
9
10 overall electrode and accommodate the volume change of metal (oxide) during the
11
12 electrochemical reactions. Nevertheless, graphene sheets commonly suffer from random stacking
13
14 with metal (oxide) nanoparticles due to the intrinsic incompatibility of these two classes of
15
16 materials and the tendency of both materials to self-aggregate.¹³ The undefined structure of
17
18 graphene-based nanocomposites and the inhomogeneous dispersion of metals (oxides) in the
19
20 graphene matrix usually result in a reduction of the resulting electrochemical performance
21
22 including the reversible capacity and cycle stability.^{14,44} Therefore, fabrication of graphene-based
23
24 hybrid materials with well-defined structures remains an important goal. Several strategies for
25
26 the fabrication of graphene-based CCNMs with defined core-shell or sandwich-like architecture
27
28 have been established recently. Moreover, the resulting materials show promise for application
29
30 for energy storage and conversions.⁴⁰

31
32
33
34
35
36
37
38
39
40
41 The first strategy employs graphene with tunable oxygen-containing groups to induce the
42
43 growth of metal oxide or hydroxide nanocrystals.^{22,11,46,47} In 2010, the first example of this
44
45 approach demonstrated that the degree of oxidation of the graphene exerted a major influence on
46
47 nanocrystal formation by metal hydroxides or oxides during hydrothermal processing.^{22, 47}
48
49 Hence, tuning the surface chemistry of graphene substrates offers a way to control the
50
51 morphology and crystallinity of the metal hydroxide/oxide nanocrystals incorporated into these
52
53 systems, as well as the performance of the resulting CCNM (Figure 11).⁴⁷ For example, growth
54
55
56
57
58
59
60

of Ni(OH)₂ on the lightly oxidized graphene sheets generated crystalline hexagonal nanoplates with uniform size.¹² The resulting nanostructure allowed for fast charge transport between the active nanoplates and the graphene-based current collectors, resulting in a specific capacitance of 1335 F g⁻¹ at a current density of 2.8 A g⁻¹ and a stable cycling performance (Figure 11c). This performance, which is significantly better than the 339 F g⁻¹ obtained for a mechanically mixed sample of graphene and Ni(OH)₂, clearly demonstrates the impact that processing protocols can have on device performance.¹²

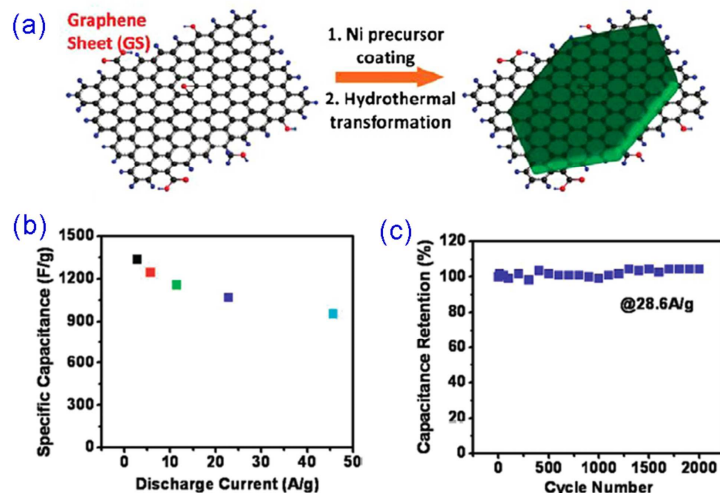
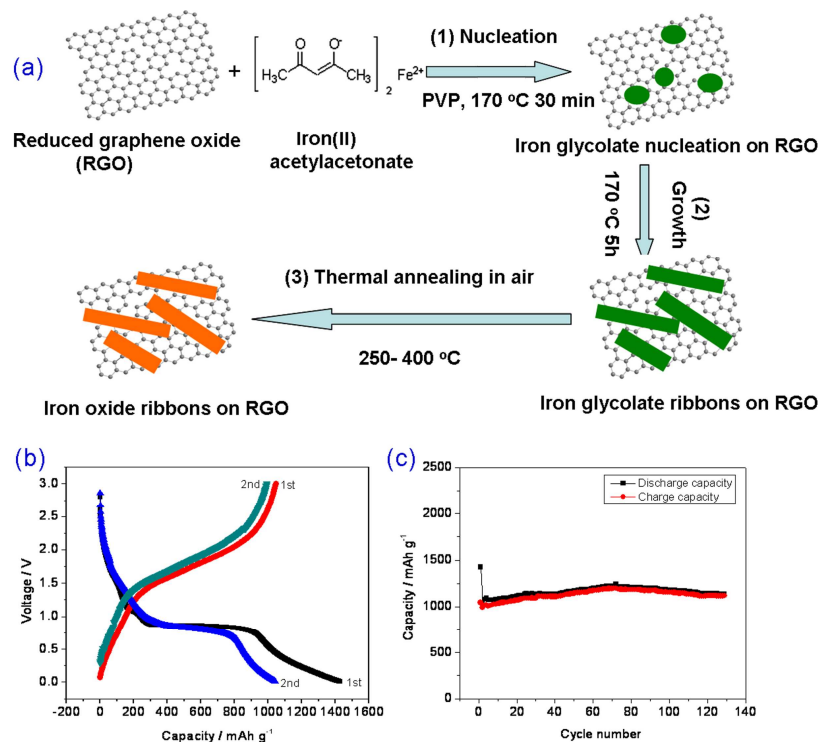


FIGURE 11. (a) Illustration of Ni(OH)₂ nanocrystal growth on lightly oxidized graphene.⁴² (b) Capacitance of Ni(OH)₂/graphene at various discharge current densities.⁹ (c) Cycle performance of Ni(OH)₂/graphene at a current density of 28.6 A g⁻¹.¹²

Recently, we also found that porous iron oxide ribbons could be fabricated by controlled growth of iron glycolate on the surface of poly(N-vinyl-2-pyrrolidone) (PVP)-functionalized graphene followed by a thermal annealing at 250°C in air (Figure 12a).⁴⁸ The resulting iron oxide

1
2
3
4 ribbons possess a large aspect ratio and porous structure, providing numerous open channels
5
6 allowing for access of electrolyte and thereby facilitating rapid diffusion of lithium ions from
7
8 electrolyte to electrode. The observed morphology also accommodates the volume change of the
9
10 iron oxides associated with lithium incorporation. As a result of these structural features, these
11
12 hybrids exhibited a reversible capacity of 1050 mAh g⁻¹ in the first 10 cycles, and over 1000
13
14 hybrids exhibited a reversible capacity of 1050 mAh g⁻¹ in the first 10 cycles, and over 1000
15
16 mAh g⁻¹ after 130 cycles (Figure 12b,12c)⁴⁸.
17
18
19
20



46 **FIGURE 12.** (a) Fabrication of of iron oxide ribbons. (b) Discharge-charge curves and (c) cycle
47
48 performance of FeO-250 ribbons at a current density of 74 mA g⁻¹.⁴⁸
49
50
51
52
53
54
55
56
57
58
59
60

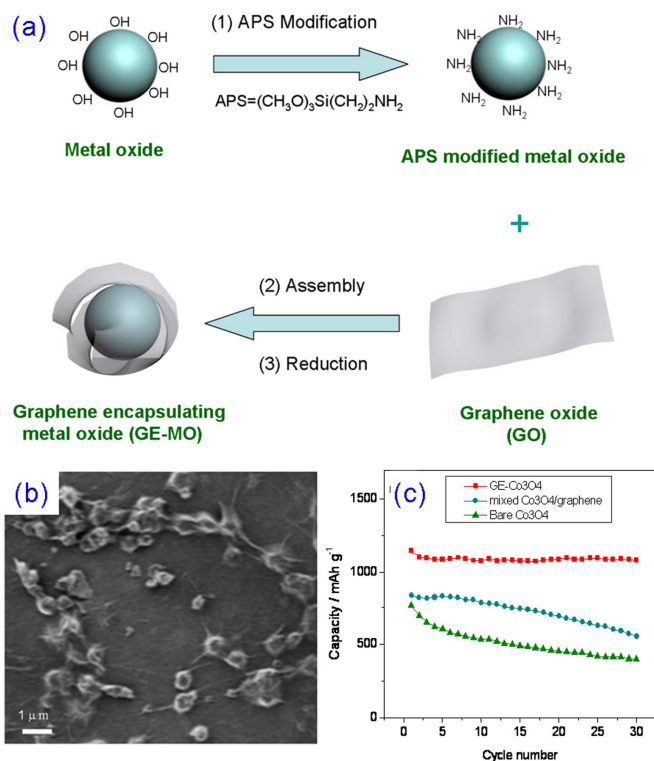


FIGURE 13. (a) Fabrication of graphene-encapsulated metal oxides. (b) TEM image of G- Co_3O_4 nanoparticles. (c) Comparison of the cycle performance of G- Co_3O_4 , mixed Co_3O_4 /graphene composite and bare Co_3O_4 electrodes at a current density of 74 mA g^{-1} .⁴⁰

The second strategy relies on encapsulation of metal (oxide) nanoparticles within individual carbon-based shells in order to completely prevent aggregation of the metal (oxide) nanoparticles. A key challenge in such an approach is to achieve both a high electrical conductivity and a high-weight fraction of the active electrode materials. Given its combination of electrical conductivity and mechanical flexibility, graphene is an ideal material for the encapsulation of metal (oxide) nanoparticles to yield core-shell CCNMs. In principle, the graphene layer can simultaneously 1) suppress the aggregation of the nanoparticles; 2)

1
2
3
4 accommodate the volume change of the metal (oxide) during the electrochemical cycling; 3)
5
6
7 yield a high metal (oxide) content in the final composite; and 4) maintain a high electrical
8
9
10 conductivity in the electrode.

11
12 A representative example of this approach is our recently reported fabrication of
13
14 graphene-encapsulated Co_3O_4 nanoparticles (G- Co_3O_4) via the co-assembly of negatively
15
16 charged graphene oxide (GO) and positively charged Co_3O_4 nanoparticles, followed by chemical
17
18 reduction of the GO (Figure 13a, 13b).⁴⁰ This G- Co_3O_4 composite showed a reversible capacity
19
20 of 1100 mAh g^{-1} in the first 10 cycles, and stable cycle performance, retaining a capacity of
21
22 $\sim 1000 \text{ mAh g}^{-1}$ after 130 cycles (Figure 13c), which is 3 times higher than that of commercial
23
24 graphite electrode ($\sim 300 \text{ mAh g}^{-1}$).⁴⁰ Following this strategy, various graphene-encapsulated
25
26 metals and metal oxides (Si, Sn, Ge, SnO_2 , Fe_2O_3) are currently being investigated as materials
27
28 for enhanced lithium storage applications.
29
30
31
32
33
34
35

36
37 The third strategy takes advantage of the 2D nature of graphene to allow for the synthesis of
38
39 graphene-based CCNMs with a sandwich-like structure. The resulting composite nanosheets
40
41 inherit the intrinsic features of graphene—high surface area, large aspect ratios, negligible
42
43 thickness and enhanced electrical conductivity—which are attractive for energy-related
44
45 applications. An example of this approach is the fabrication of graphene-based mesoporous silica
46
47 (G-silica) nanosheets, in which graphene sheets are separated by mesoporous silica layers. The
48
49 synthesis uses cetyltrimethyl ammonium bromide (CTAB)-modified graphene oxide sheets as a
50
51 template and tetraethylorthosilicate as the silica precursor (Figure 14). The resulting G-silica
52
53 nanosheets possess a large aspect ratio, mesoporous structure, high surface area, and high
54
55
56
57
58
59
60

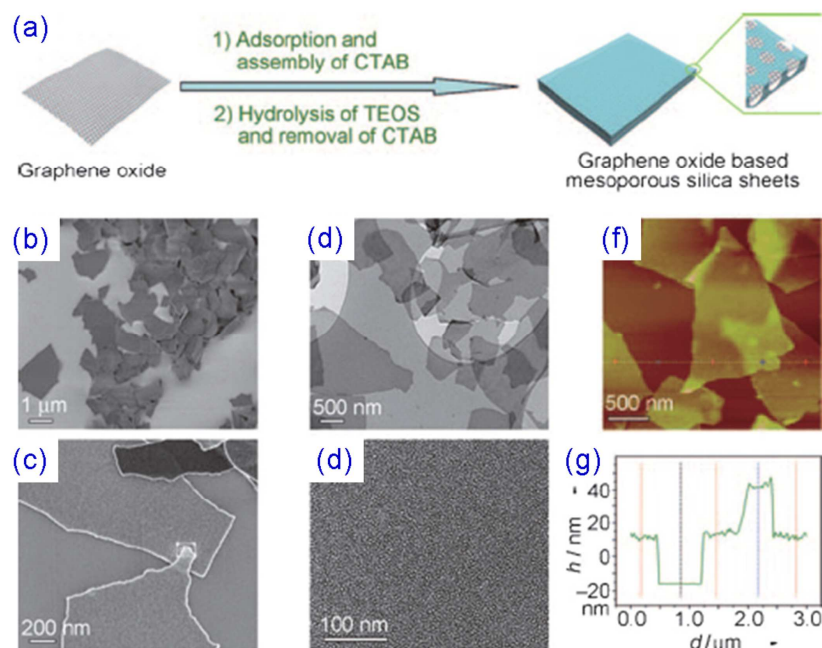


FIGURE 14. (a) Illustration of the fabrication of graphene oxide based mesoporous silica (G-silica) sheets, (b,c) FE-SEM and (d,e) TEM images of G-silica. (f) Representative AFM image and (g) corresponding thickness analysis taken around the white line in (f).¹³

monodispersity. This approach also allows for the generation of composite nanosheets incorporating layers of materials like mesoporous carbon, metal, and metal oxide sheets on graphene. For instance, graphene based mesoporous titania (G-TiO₂) nanosheets were fabricated by treating preformed G-silica nanosheets with (NH₄)₂TiF₆.⁴⁹ The numerous open channels in the resulting G-TiO₂ allow access of electrolyte, facilitating the ultrafast diffusion of lithium ions during the cycling processes. Moreover, the graphene layer within each nanosheet acts as mini-current collectors, aiding fast electron transport in the electrode. As a result, a high-rate capability of 123 mAh g⁻¹ at 10 C and good cycle performance could be achieved for the G-TiO₂

nanosheets (Figure 15). For comparison, TiO_2 nanosheets without graphene show a capacity of only approximately 40 mAh g^{-1} .

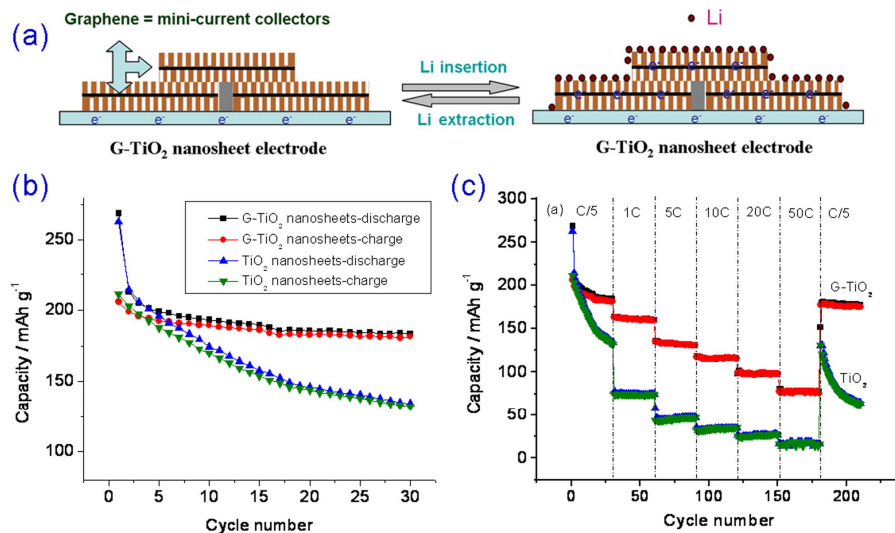
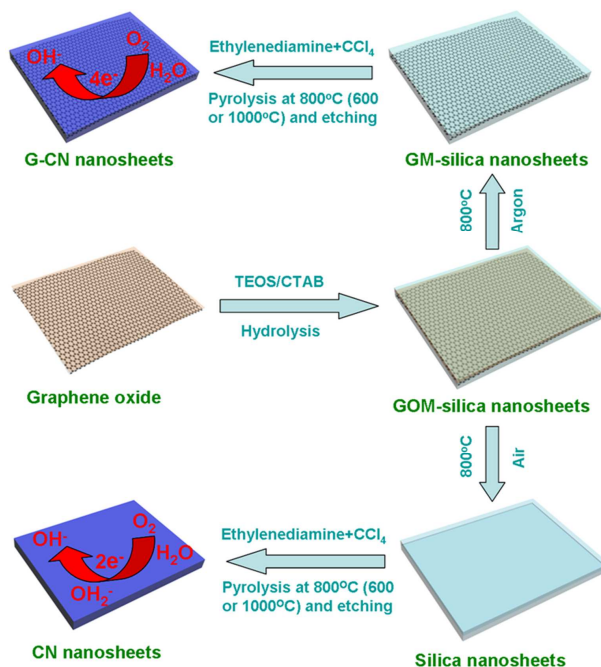


FIGURE 15. (a) Lithium insertion and extraction in G-TiO₂ nanosheets,. (b) Initial charge-discharge curves of G-TiO₂ nanosheets at a current density of C/5. (c) Cycle performance of G-TiO₂ and TiO₂ nanosheets.⁴⁹

Sandwich-like graphene carbon nitride (G-CN) nanosheets were produced from G-silica templates using ethylenediamine and carbon tetrachloride as the CN precursors (Figure 16).⁵⁰ The resulting G-CN nanosheets possessed a nitrogen content of approximately 20 wt%, a thicknesses of about 18 nm and high surface area up to $542 \text{ m}^2 \text{ g}^{-1}$.⁵⁰ These features allowed ready access of oxygen to the catalyst surface and facilitated the rapid diffusion of electrons through the electrode during the ORR, providing excellent electrocatalytic activity in alkaline

1
2
3
4 solution.⁵⁰ The current density, electron-transfer number, durability, and selectivity were superior
5
6
7 to those observed for CN sheets without graphene or commercially available Pt–C catalysts.
8



31
32 **FIGURE 16.** Fabrication of carbon nitride (G-CN) and CN nanosheets for the ORR.⁵⁰
33
34

35 6. Conclusions and Prospects

36
37

38
39 In summary, CCNMs are playing an increasingly important role in improving the performance
40 of electrochemical energy storage and conversion devices owing to their favorable nanoscale
41 structural features and the intrinsic synergy between the two components of the systems. In this
42 Account, we have summarized recent representative advancements toward the controlled
43 synthesis of CCNMs as a function of the carbon precursor. The relationship between the
44 structures of the resulting CCNMs and their electrochemical performance has also been
45 highlighted in this context. Although a variety of CCNMs with tunable structures and
46
47
48
49
50
51
52
53
54
55
56
57
58
59
60

1
2
3
4 compositions have been fabricated via the methods discussed, these results are only the
5
6 beginning. It seems clear that the continued development of these approaches will yield new
7
8 multifunctional CCNMs with enhanced electrochemical properties suitable for application in
9
10 energy storage and conversion devices. It also seems reasonable that these materials could make
11
12 miniaturized devices, such as nanoscale batteries, possible.
13
14
15

16
17 With regard to the three “molecular” approaches (low molecular weight organic or
18
19 organometallic systems, aromatic polymer networks and discotic molecules), a deeper
20
21 understanding regarding the relationship between the structure and physical properties of the
22
23 precursors and those of the product CCNM will be required. However, even at this early stage a
24
25 few initial conclusions seem warranted. For example, use of low molecular weight molecular
26
27 precursors or aromatic polymer networks typically gives rise to an amorphous carbon component
28
29 in the CCNM. In contrast, use of discotic precursors typically yields a graphitic matrix.
30
31
32
33
34
35

36 For the graphene-based hybrids, control of bulk morphology and the nanostructure of the other
37
38 functional components on the graphene surface are critical issues. While the successful
39
40 fabrication of graphene-based CCNMs including graphene-nanocrystal composites, core-shell
41
42 graphene-encapsulated metal (oxide) nanoparticles and sandwich-like graphene-metal oxide
43
44 nanosheets has been achieved, this area of research is still in its infancy and many challenges
45
46 remain. In particular, the obstacle of the intrinsic incompatibility between graphene and
47
48 inorganic materials needs to be resolved in order to gain fuller access to graphene-based CCNMs
49
50 with desirable nanoscale architectures in a controlled manner. Given the rapid development of
51
52 this research direction, one can expect that additional graphene-based hybrid materials
53
54
55
56
57
58
59
60

1
2
3
4 incorporating a variety of multifunctional components will soon be readily available. Such an
5
6 achievement will, in our view, result in a range of novel electrode materials for the next
7
8 generation energy storage and conversion devices.
9
10

11 12 13 14 15 ACKNOWLEDGMENT

16
17
18 This work was financially supported by ERC grant on NANOGRAPH, the Max Planck Society
19
20 through the program ENERCHEM, DFG Priority Program SPP 1459, BMBF LiBZ Project, and
21
22 ESF Project GOSPEL (Ref Nr: 09-EuroGRAPHENE-FP-001), EU Project MOLESOL and
23
24 GENIUS. REB acknowledges the fellowship support from the Alexander von Humboldt
25
26 Foundation and the German Academic Exchange Service.
27
28
29
30
31
32

33 34 35 BIOGRAPHICAL INFORMATION

36
37
38 **Dr. Shubin Yang** received his PhD from Beijing University of Chemical Technology in 2008
39
40 after carrying out a thesis on high-performance lithium ion batteries under the guidance of Prof.
41
42 Huaihe Song. And then he pursued postdoctoral research with Prof. K. Müllen at Max-Planck
43
44 Institute for Polymer Research. His current research interests involve in carbon-rich materials for
45
46 energy storage and conversions.
47
48
49

50
51
52 **Prof. Robert E. Bachman** received his PhD degree from Rice University in 1994 under the
53
54 direction of Prof. Kenton Whitmire. After an Alexander von Humboldt (AvH) post-doctoral
55
56

1
2
3
4 fellowship at the Technical University München with Prof. Hubert Schmidbaur, Prof. Bachman
5
6
7 joined the faculty of Georgetown University in 1995. He moved to The University of the South
8
9
10 in 2001 and was promoted to Professor in 2010. Prof. Bachman spent 2011-12 on sabbatical at
11
12 the Max Planck Institute for Polymer Research. His current research interests focus on
13
14 self-assembly of inorganic complexes and soft inorganic materials.
15
16

17
18 **Prof. Xinliang Feng** joined the group of Prof. K. Müllen at the Max Planck Institute for Polymer
19
20 Research (MPIP) and obtained his PhD degree in April 2008. Since December 2007, he was
21
22 appointed as project leader in MPIP. He became a Professor at Shanghai Jiao Tong University in
23
24 2011. His current scientific interests include the conjugated oligomers and polymers, graphene,
25
26 carbon-rich molecules and materials for electronic and energy-related applications.
27
28
29

30
31
32 **Prof. Klaus Müllen** received his PhD in 1972 at the University of Basel (Switzerland). He
33
34 pursued postdoctoral research with Prof. J.F.M. Oth at ETH Zurich, where he obtained his
35
36 habilitation in 1977. After working as a Professor of Organic Chemistry at the universities of
37
38 Cologne and Mainz, he became a scientific member of the Max Planck Society in 1989 and was
39
40 appointed Director of the Department for Synthetic Chemistry at MPIP. His current research
41
42 focus lies on synthetic macromolecular chemistry and materials science.
43
44
45
46
47

48 49 **Corresponding Author**

50 *muellen@mpip-mainz.mpg.de, feng@mpip-mainz.mpg.de
51
52
53
54

55 56 **Notes**

57
58
59
60

1
2
3
4 The authors declare no competing financial interest
5
6
7
8

9
10 REFERENCES
11

- 12
13 1. Maier, J., Nanoionics: ion transport and electrochemical storage in confined systems. *Nature Mater.*
14
15 **2005**, *4* (11), 805-815.
16
17
18
19 2. Guo, Y. G.; Hu, J. S.; Wan, L. J., Nanostructured materials for electrochemical energy conversion and
20
21 storage devices. *Adv. Mater.* **2008**, *20* (15), 2878-2887.
22
23
24
25 3. Recham, N.; Chotard, J. N.; Dupont, L.; Delacourt, C.; Walker, W.; Armand, M.; Tarascon, J. M., A 3.6
26
27 V lithium-based fluorosulphate insertion positive electrode for lithium-ion batteries. *Nature Mater.*
28
29 **2010**, *9* (1), 68-74.
30
31
32
33 4. Taberna, L.; Mitra, S.; Poizot, P.; Simon, P.; Tarascon, J. M., High rate capabilities Fe₃O₄-based Cu
34
35 nano-architected electrodes for lithium-ion battery applications. *Nature Mater.* **2006**, *5* (7), 567-573.
36
37
38
39 5. Magasinski, A.; Dixon, P.; Hertzberg, B.; Kvit, A.; Ayala, J.; Yushin, G., High-performance lithium-ion
40
41 anodes using a hierarchical bottom-up approach. *Nature Mater.* **2010**, *9* (4), 353-358.
42
43
44
45 6. Wessells, C. D.; Huggins, R. A.; Cui, Y., Copper hexacyanoferrate battery electrodes with long cycle
46
47 life and high power. *Nature Commun.* **2011**, *2*.
48
49
50
51
52
53
54
55
56
57
58
59
60

- 1
2
3
4 7. Yang, S. B.; Feng, X. L.; Zhi, L. J.; Cao, Q. A.; Maier, J.; Müllen, K., Nanographene-Constructed
5
6
7 Hollow Carbon Spheres and Their Favorable Electroactivity with Respect to Lithium Storage. *Adv.*
8
9 *Mater.* **2010**, *22* (7), 838-842.
10
- 11
12
13 8. Hou, J. B.; Shao, Y. Y.; Ellis, M. W.; Moore, R. B.; Yi, B. L., Graphene-based electrochemical energy
14
15 conversion and storage: fuel cells, supercapacitors and lithium ion batteries. *PCCP* **2011**, *13* (34),
16
17 15384-15402.
18
19
- 20
21
22 9. Zhang, H. L.; Morse, D. E., Kinetically controlled catalytic synthesis of highly dispersed
23
24 metal-in-carbon composite and its electrochemical behavior. *J. Mater. Chem.* **2009**, *19* (47), 9006-9011.
25
26
27
- 28
29
30 10. Yang, S. B.; Song, H. H.; Chen, X. H., Electrochemical performance of expanded mesocarbon
31
32 microbeads as anode material for lithium-ion batteries. *Electrochem. Commun.* **2006**, *8* (1), 137-142.
33
- 34
35
36 11. Qu, Q. T.; Yang, S. B.; Feng, X. L., 2D Sandwich-like Sheets of Iron Oxide Grown on Graphene as
37
38 High Energy Anode Material for Supercapacitors. *Adv. Mater.* **2011**, *23* (46), 5574-5580.
39
- 40
41
42 12. Wang, H. L.; Casalongue, H. S.; Liang, Y. Y.; Dai, H. J., Ni(OH)(2) Nanoplates Grown on Graphene as
43
44 Advanced Electrochemical Pseudocapacitor Materials. *J. Am. Chem. Soc.* **2010**, *132* (21), 7472-7477.
45
- 46
47
48 13. Yang, S. B.; Feng, X. L.; Wang, L.; Tang, K.; Maier, J.; Müllen, K., Graphene-Based Nanosheets with a
49
50 Sandwich Structure. *Angew. Chem. Int. Ed.* **2010**, *49* (28), 4795-4799.
51
52
53
54
55
56
57
58
59
60

- 1
2
3
4 14. Yang, S. B.; Cui, G. L.; Pang, S. P.; Cao, Q.; Kolb, U.; Feng, X. L.; Maier, J.; Müllen, K., Fabrication of
5
6
7 Cobalt and Cobalt Oxide/Graphene Composites: Towards High-Performance Anode Materials for
8
9
10 Lithium Ion Batteries. *Chemsuschem* **2010**, *3* (2), 236-239.
11
12
13 15. Zhi, L. J.; Müllen, K., A bottom-up approach from molecular nanographenes to unconventional carbon
14
15
16 materials. *J. Mater. Chem.* **2008**, *18* (13), 1472-1484.
17
18
19 16. Liang, Y. Y.; Schwab, M. G.; Shu, J.; Graf, R.; Spiess, H. W.; Feng, X. L.; Müllen, K., Template-Free
20
21
22 Fabrication of Nitrogen-Enriched Mesoporous Carbons from Schiff Base Networks and Applications in
23
24
25 High-Performance Electrochemical Capacitors. *Nature Mater.* **2012** (SUBMITTED).
26
27
28 17. Zhi, L.; Wang, J. J.; Cui, G. L.; Kastler, M.; Schmaltz, B.; Kolb, U.; Jonas, U.; Müllen, K., From
29
30
31 well-defined carbon-rich precursors to monodisperse carbon particles with hierarchic structures. *Adv.*
32
33
34 *Mater.* **2007**, *19* (14), 1849-1853.
35
36
37 18. Cui, G. L.; Gu, L.; Zhi, L. J.; Kaskhedikar, N.; van Aken, P. A.; Müllen, K.; Maier, J., A
38
39
40 Germanium-Carbon Nanocomposite Material for Lithium Batteries. *Adv. Mater.* **2008**, *20* (16),
41
42
43 3079-3083.
44
45
46 19. Cui, G. L.; Hu, Y. S.; Zhi, L. J.; Wu, D. Q.; Lieberwirth, I.; Maier, J.; Müllen, K., A one-step approach
47
48
49 towards carbon-encapsulated hollow tin nanoparticles and their application in lithium batteries. *Small*
50
51
52 **2007**, *3* (12), 2066-2069.
53
54
55
56
57
58
59
60

- 1
2
3
4 20. Schwab, M. G.; Fassbender, B.; Spiess, H. W.; Thomas, A.; Feng, X. L.; Müllen, K., Catalyst-free
5
6 Preparation of Melamine-Based Microporous Polymer Networks through Schiff Base Chemistry. *J. Am.*
7
8
9
10 *Chem. Soc.* **2009**, *131* (21), 7216-7217.
- 11
12
13 21. Zhi, L. J.; Wu, J. S.; Li, J. X.; Kolb, U.; Müllen, K., Carbonization of dislike molecules in porous
14
15 alumina membranes: Toward carbon nanotubes with controlled graphene-layer orientation. *Angew.*
16
17
18 *Chem. Int. Ed.* **2005**, *44* (14), 2120-2123.
- 19
20
21
22 22. Wang, H. L.; Yang, Y.; Liang, Y. Y.; Cui, L. F.; Casalongue, H. S.; Li, Y. G.; Hong, G. S.; Cui, Y.; Dai,
23
24 H. J., LiMn(1-x)Fe(x)PO(4) Nanorods Grown on Graphene Sheets for Ultrahigh-Rate-Performance
25
26
27
28
29
30
31
32
33
34
35
36
37
38
39
40
41
42
43
44
45
46
47
48
49
50
51
52
53
54
55
56
57
58
59
60
23. Cui, G. L.; Zhi, L. J.; Thomas, A.; Lieberwirth, I.; Kolb, U.; Müllen, K., A novel approach towards
carbon-Ru electrodes with mesoporosity for supercapacitors. *Chemphyschem* **2007**, *8* (7), 1013-1015.
24. Kim, H.; Popov, B. N., Characterization of hydrous ruthenium oxide/carbon nanocomposite
supercapacitors prepared by a colloidal method. *J. Power Sources* **2002**, *104* (1), 52-61.
25. Zhi, L. J.; Hu, Y. S.; El Hamaoui, B.; Wang, X.; Lieberwirth, I.; Kolb, U.; Maier, J.; Müllen, K.,
Precursor-controlled formation of novel carbon/metal and carbon/metal oxide nanocomposites. *Adv.*
Mater. **2008**, *20* (9), 1727-1731.
26. Kim, H.; Cho, J., Superior Lithium Electroactive Mesoporous Si@Carbon Core-Shell Nanowires for
Lithium Battery Anode Material. *Nano Lett.* **2008**, *8* (11), 3688-3691.

- 1
2
3
4 27. Kim, H.; Han, B.; Choo, J.; Cho, J., Three-Dimensional Porous Silicon Particles for Use in
5
6 High-Performance Lithium Secondary Batteries. *Angew. Chem. Int. Ed.* **2008**, *47* (52), 10151-10154.
7
8
9
10 28. Seo, M. H.; Park, M.; Lee, K. T.; Kim, K.; Kim, J.; Cho, J., High performance Ge nanowire anode
11
12 sheathed with carbon for lithium rechargeable batteries. *Energy Environ. Sci.* **2011**, *4* (2), 425-428.
13
14
15
16 29. Lee, H.; Cho, J., Sn(78)Ge(22)@carbon core-shell nanowires as fast and high-capacity lithium storage
17
18 media. *Nano Lett.* **2007**, *7* (9), 2638-2641.
19
20
21
22 30. Kwon, Y.; Kim, H.; Doo, S. G.; Cho, J. H., Sn_{0.9}Si_{0.1}/carbon core-shell nanoparticles for high-density
23
24 lithium storage materials. *Chem. Mater.* **2007**, *19* (5), 982-986.
25
26
27
28 31. Lee, J. S.; Wang, X. Q.; Luo, H. M.; Baker, G. A.; Dai, S., Facile Ionothermal Synthesis of Microporous
29
30 and Mesoporous Carbons from Task Specific Ionic Liquids. *J. Am. Chem. Soc.* **2009**, *131* (13),
31
32 4596-4597.
33
34
35
36
37 32. Yang, W.; Fellingner, T. P.; Antonietti, M., Efficient Metal-Free Oxygen Reduction in Alkaline Medium
38
39 on High-Surface-Area Mesoporous Nitrogen-Doped Carbons Made from Ionic Liquids and
40
41 Nucleobases. *J. Am. Chem. Soc.* **2011**, *133* (2), 206-209.
42
43
44
45
46 33. Liang, Y. Y.; Feng, X. L.; Zhi, L. J.; Kolb, U.; Müllen, K., A simple approach towards one-dimensional
47
48 mesoporous carbon with superior electrochemical capacitive activity. *Chem. Commun.* **2009**, *7*,
49
50 809-811.
51
52
53
54
55
56
57
58
59
60

- 1
2
3
4 34. Liang, Y. Y.; Schwab, M. G.; Zhi, L. J.; Mugnaioli, E.; Kolb, U.; Feng, X. L.; Müllen, K., Direct Access
5
6
7 to Metal or Metal Oxide Nanocrystals Integrated with One-Dimensional Nanoporous Carbons for
8
9 Electrochemical Energy Storage. *J. Am. Chem. Soc.* **2010**, *132* (42), 15030-15037.
10
11
12
13 35. Feng, X. L.; Liang, Y. Y.; Zhi, L. J.; Thomas, A.; Wu, D. Q.; Lieberwirth, I.; Kolb, U.; Müllen, K.,
14
15 Synthesis of Microporous Carbon Nanofibers and Nanotubes from Conjugated Polymer Network and
16
17 Evaluation in Electrochemical Capacitor. *Adv. Funct. Mater.* **2009**, *19* (13), 2125-2129.
18
19
20
21 36. Segade, A.; Castella, M.; Lopez-Calahorra, F.; Velasco, D., Synthesis and characterization of
22
23
24 unsymmetrically beta-substituted porphyrin liquid crystals: Influence of the chemical structure on the
25
26
27 mesophase ordering. *Chem. Mater.* **2005**, *17* (21), 5366-5374.
28
29
30
31 37. Sienkowska, M. J.; Monobe, H.; Kaszynski, P.; Shimizu, Y., Photoconductivity of liquid crystalline
32
33
34 derivatives of pyrene and carbazole. *J. Mater. Chem.* **2007**, *17* (14), 1392-1398.
35
36
37 38. Wu, J. S.; Watson, M. D.; Zhang, L.; Wang, Z. H.; Müllen, K.,
38
39 Hexakis(4-iodophenyl)-peri-hexabenzocoronene - A versatile building block for highly ordered discotic
40
41
42 liquid crystalline materials. *J. Am. Chem. Soc.* **2004**, *126* (1), 177-186.
43
44
45
46 39. Liu, R. L.; Wu, D. Q.; Feng, X. L.; Müllen, K., Nitrogen-Doped Ordered Mesoporous Graphitic Arrays
47
48
49 with High Electrocatalytic Activity for Oxygen Reduction. *Angew. Chem. Int. Ed.* **2010**, *49* (14),
50
51
52 2565-2569.
53
54
55
56
57
58
59
60

- 1
2
3
4 40. Yang, S. B.; Feng, X. L.; Ivanovici, S.; Müllen, K., Fabrication of Graphene-Encapsulated Oxide
5
6 Nanoparticles: Towards High-Performance Anode Materials for Lithium Storage. *Angew. Chem. Int. Ed.*
7
8
9 **2010**, *49* (45), 8408-8411.
10
11
12
13 41. Novoselov, K. S.; Geim, A. K.; Morozov, S. V.; Jiang, D.; Katsnelson, M. I.; Grigorieva, I. V.;
14
15 Dubonos, S. V.; Firsov, A. A., Two-dimensional gas of massless Dirac fermions in graphene. *Nature*
16
17 **2005**, *438* (7065), 197-200.
18
19
20
21
22 42. El-Kady, M. F.; Strong, V.; Dubin, S.; Kaner, R. B., Laser Scribing of High-Performance and Flexible
23
24 Graphene-Based Electrochemical Capacitors. *Science* **2012**, *335* (6074), 1326-1330.
25
26
27
28 43. Yoo, E.; Okata, T.; Akita, T.; Kohyama, M.; Nakamura, J.; Honma, I., Enhanced Electrocatalytic
29
30 Activity of Pt Subnanoclusters on Graphene Nanosheet Surface. *Nano Lett.* **2009**, *9* (6), 2255-2259.
31
32
33
34 44. Paek, S. M.; Yoo, E.; Honma, I., Enhanced Cyclic Performance and Lithium Storage Capacity of
35
36 SnO(2)/Graphene Nanoporous Electrodes with Three-Dimensionally Delaminated Flexible Structure.
37
38 *Nano Lett.* **2009**, *9* (1), 72-75.
39
40
41
42
43 45. Wu, Z. S.; Ren, W. C.; Wen, L.; Gao, L. B.; Zhao, J. P.; Chen, Z. P.; Zhou, G. M.; Li, F.; Cheng, H. M.,
44
45 Graphene Anchored with Co(3)O(4) Nanoparticles as Anode of Lithium Ion Batteries with Enhanced
46
47 Reversible Capacity and Cyclic Performance. *Acs Nano* **2010**, *4* (6), 3187-3194.
48
49
50
51
52 46. Wang, H. L.; Cui, L. F.; Yang, Y. A.; Casalongue, H. S.; Robinson, J. T.; Liang, Y. Y.; Cui, Y.; Dai, H.
53
54 J., Mn(3)O(4)-Graphene Hybrid as a High-Capacity Anode Material for Lithium Ion Batteries. *J. Am.*
55
56 *Chem. Soc.* **2010**, *132* (40), 13978-13980.
57
58
59
60

- 1
2
3
4 47. Wang, H. L.; Robinson, J. T.; Diankov, G.; Dai, H. J., Nanocrystal Growth on Graphene with Various
5
6 Degrees of Oxidation. *J. Am. Chem. Soc.* **2010**, *132* (10), 3270-3271.
7
8
9
10 48. Yang, S. B.; Sun, Y.; Chen, L.; Hernandez, Y.; Feng, X. L.; Müllen, K., Porous Iron Oxide Ribbons
11
12 Grown on Graphene for High-Performance Lithium Storage. *Scientific Report* **2012**, *2*, 427
13
14
15
16 49. Yang, S. B.; Feng, X. L.; Müllen, K., Sandwich-Like, Graphene-Based Titania Nanosheets with High
17
18 Surface Area for Fast Lithium Storage. *Adv. Mater.* **2011**, *23* (31), 3575-3579.
19
20
21
22 50. Yang, S. B.; Feng, X. L.; Wang, X. C.; Müllen, K., Graphene-Based Carbon Nitride Nanosheets as
23
24 Efficient Metal-Free Electrocatalysts for Oxygen Reduction Reactions. *Angew. Chem. Int. Ed.* **2011**, *50*
25
26
27
28 (23), 5339-5343.
29
30
31
32
33
34
35
36
37
38
39
40
41
42
43
44
45
46
47
48
49
50
51
52
53
54
55
56
57
58
59
60